Model of driver overacceleration causing breakdown in vehicular traffic

Boris S. Kerner
Physics of Transport and Traffic, University of Duisburg-Essen, 47048 Duisburg, Germany

(Received 13 September 2023; accepted 20 November 2023; published 22 December 2023)

We introduce a mathematical approach for the description of driver overacceleration in a microscopic traffic flow model. The model, in which no driver overreaction occurs, explains the empirical nucleation nature of traffic breakdown.

DOI: 10.1103/PhysRevE.108.064305

I. INTRODUCTION

Traffic breakdown is a transition from free flow to congested vehicular traffic occurring mostly at bottlenecks. Between 1958 and 1961 Herman, Gazis, Montroll, Potts, Rothery, and Chandler [1–4] as well as Kometani and Sasaki [5–7] assumed that the cause of the breakdown is driver *overreaction* on the deceleration of the preceding vehicle: Due to a delayed deceleration of the vehicle resulting from a driver reaction time, the driver decelerates stronger than it is needed to avoid vehicle collisions. In other words, driver overreaction causes vehicle overdeceleration. Due to overdeceleration, the vehicle speed becomes less than the speed of the preceding vehicle. If driver overreaction is realized for all following drivers, then traffic instability occurs [1–17]. The traffic instability leads to a wide moving jam (J) formation in free flow (F) called an F → J transition [18]. This classical traffic instability is currently a theoretical basic of standard traffic theory (e.g., [8–17,19–28]).

However, rather than the F → J transition, in real field (empirical) traffic data traffic breakdown is a phase transition from free flow to synchronized flow (S) (F → S transition) [29–33]; the empirical traffic breakdown (empirical F → S transition) exhibits the nucleation nature [Fig. 1(a)][1]. To explain the empirical nucleation nature of the F → S transition, three-phase traffic theory was introduced [29–32], in which there are three phases: free flow (F), synchronized flow (S), and wide moving jam (J), where the phases S and J belong to congested traffic.

Contrary to standard traffic theory in which driver overreaction should be responsible for traffic breakdown [1–28], it is assumed in three-phase traffic theory [29–32,40] that the empirical nucleation nature of traffic breakdown (F → S transition) is caused by a discontinuity in the probability of driver acceleration occurring when free flow transforms into synchronized flow [Fig. 1(b)]: In free flow, drivers can accelerate from car following at a lower speed to a higher speed with a larger probability than it occurs in synchronized flow. Driver acceleration that probability exhibits the discontinuity when free flow transforms into synchronized flow is called driver *overacceleration*, to distinguish driver overacceleration from "usual" driver acceleration that does not show a discontinuous character[2].

The behavioral origin of driver overacceleration is related to the wish of drivers to move in free flow. The discontinuity in the probability of driver overacceleration [Fig. 1(b)], i.e., the discontinuous character of driver overacceleration is explained as follows (see for more details Sec. VII): At small space gaps between vehicles and a low speed in synchronized flow, vehicles prevent each other to accelerate from synchronized flow to free flow; contrarily, due to larger space gaps in free flow at the same flow rate, drivers can easily accelerate from a local speed decrease. The discontinuous character of driver overacceleration can lead to an S → F instability in synchronized flow [31,32,41].

Contrary to the classical traffic instability that is a growing wave of a local *decrease* in the vehicle speed [1–28], the S → F instability is a growing wave of a local *increase* in the speed [31,32,41]. Microscopic three-phase traffic flow models [42] that simulate the empirical nucleation nature of traffic breakdown [Fig. 1(a)] show also the classical traffic instability leading to a wide moving jam emergence in synchronized flow. In these complex traffic flow models [42,43], both driver overacceleration and driver overreaction are important.

Thus, up to now there has been no mathematical model of driver overacceleration on a single-lane road that can explain the empirical nucleation nature of traffic breakdown (F → S transition) at bottlenecks solely through driver overacceleration, i.e., without the effect of driver overreaction. The

[1]We do not consider classical Lighthill-Whitham-Richards (LWR) model of traffic breakdown [35–39] because the LWR model cannot explain the empirical nucleation nature of traffic breakdown [29–32].

[2]In [40], the discontinuity in the probability of overacceleration shown in Fig. 1(b) has been considered for the case of lane-changing on multi-lane roads and it has been called "probability of passing" (see Fig. 5.7(b) of Ref. [29]). First mathematical approaches for simulation of overacceleration for both single-lane and multi-lane roads have been introduced in Kerner-Klenov stochastic and deterministic ATD (acceleration time delay) microscopic models as well as in KKW (Kerner-Klenov-Wolf) and KKSW (Kerner-Klenov-Schreckenberg-Wolf) cellular automaton models developed in the framework of three-phase traffic theory (see explanations in Chap. 11 of [30] and Appendixes A and B of [31]).

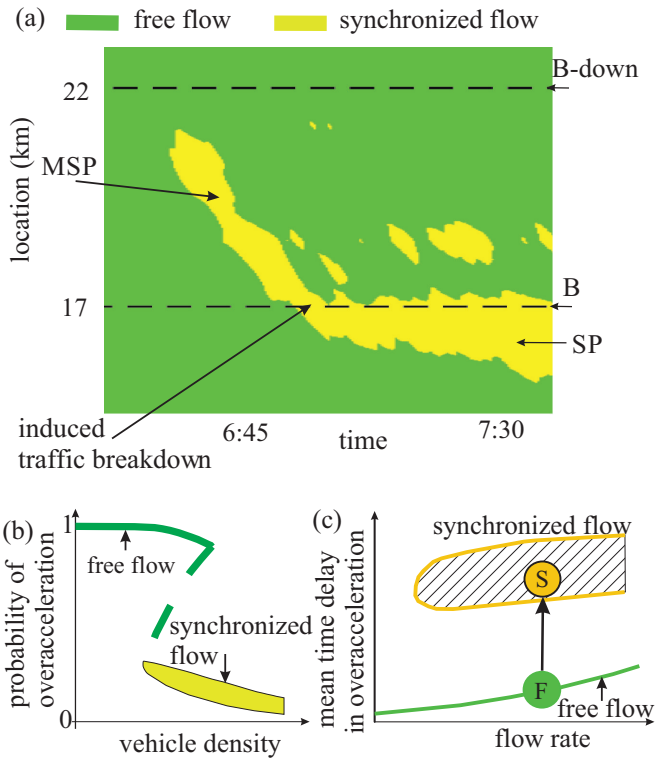

FIG. 1. Empirical nucleation nature of traffic breakdown (F → S transition) at bottlenecks (a) and a hypothesis of three-phase traffic theory for the discontinuous character of driver overacceleration (b), (c) [40]. (a) Speed data presented in space and time with averaging method described in Sec. C.2 of Ref. [34] were measured with road detectors installed along road: A moving synchronized flow pattern (MSP) that has emerged at downstream bottleneck (B-down) while propagating upstream induces F → S transition (induced traffic breakdown) leading to emergence of a synchronized flow pattern (SP) at upstream bottleneck (B); adapted from [29–32]. (b), (c) Qualitative vehicle density dependence of driver overacceleration probability per a time interval (b) and equivalent presentation of (b) as a discontinuous flow-rate dependence of the mean time delay in driver overacceleration (c). F and S are states of free flow and synchronized flow, respectively.

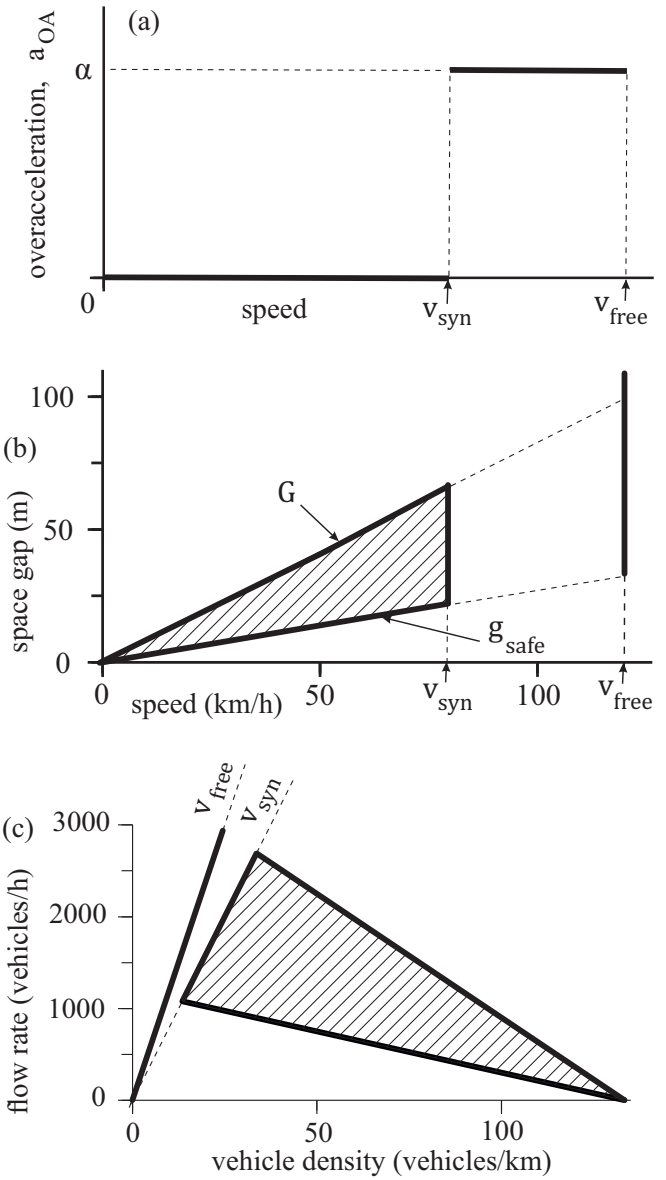

FIG. 2. Qualitative speed dependence of driver overacceleration $a_{OA}(v)$ in Eq. (1) (a) as well as steady states of model (2)–(5) in space-gap–speed (b) and flow–density (c) planes (dashed 2D-regions are related to steady states of synchronized flow). $v_{free} = 120$ km/h, $\tau_{safe} = 1$ s, $\tau_G = 3$ s, $v_{syn} = 80$ km/h, $d = 7.5$ m.

introduction of such a model for driver overacceleration in a road lane is the objective of this paper.

The paper is organized as follows: In Sec. II we introduce a mathematical model of driver overacceleration on a single-lane road (Sec. II A), present a microscopic deterministic traffic flow model incorporating this overacceleration model (Sec. II B), and consider the physics of the model (Sec. II C). Simulations of the nucleation nature of traffic breakdown (F → S transition) and of the S → F instability are presented in Secs. III and IV, respectively. In Sec. V we study features of traffic patterns resulting from traffic breakdown. In Sec. VI, based on model simulations we show that there is no driver overreaction in the traffic flow model. The behavioral origin of the discontinuous character of driver overacceleration in a road lane is considered in Sec. VII. In our discussion, Sec. VIII, we consider the agreement of the overacceleration model with real field (empirical) traffic data (Sec. VIII A), analyze possible changes in model parameters at which driver overreaction becomes possible at a low enough synchronized flow speed that results in the emergence of a wide moving jam in synchronized flow (Sec. VIII B), and formulate conclusions (Sec. VIII C).

II. MODEL

A. Driver overacceleration in road lane

Here we introduce a mathematical approach for driver overacceleration a_{OA} [Fig. 2(a)]:

$$a_{OA} = \alpha\Theta(v - v_{syn}). \tag{1}$$

Equation (1) satisfies the hypothesis of three-phase traffic theory about the discontinuous character of driver overaccel-

eration [Figs. 1(b) and 1(c)] [29–32,40]. In (1), v is the vehicle speed, where $0 \leqslant v \leqslant v_{\text{free}}$, v_{free} is a maximum vehicle speed; α is a maximum driver overacceleration; $\Theta(z) = 0$ at $z < 0$ and $\Theta(z) = 1$ at $z \geqslant 0$; and v_{syn} is a given synchronized flow speed ($v_{\text{syn}} < v_{\text{free}}$).

B. Microscopic deterministic traffic flow model

Based on Eq. (1), we develop a microscopic traffic flow model, in which vehicle acceleration or deceleration a in a road lane is described by a system of equations:

$$a = K_{\Delta v}\Delta v + a_{\text{OA}} \quad \text{at} \quad g_{\text{safe}} \leqslant g \leqslant G, \tag{2}$$

$$a = a_{\max} \quad \text{at} \quad g > G, \tag{3}$$

$$a = a_{\text{safety}}(g, v, v_\ell) \quad \text{at} \quad g < g_{\text{safe}}, \tag{4}$$

where driver overacceleration a_{OA} is given by Eq. (1); g is a space gap to the preceding vehicle, $g = x_\ell - x - d$, where x and x_ℓ are, respectively, the coordinates of the vehicle and the preceding vehicle and d is the vehicle length; $\Delta v = v_\ell - v$, v_ℓ is the speed of the preceding vehicle; $K_{\Delta v}$ is a positive dynamic coefficient; $a_{\max}$ is a maximum vehicle acceleration; G is a synchronization space gap, $G = v\tau_{\text{G}}$, τ_{G} is a synchronization time headway; g_{safe} is a safe space gap, $g_{\text{safe}} = v\tau_{\text{safe}}$ [Figs. 2(b) and 2(c)], where τ_{safe} is a safe time headway; and $a_{\text{safety}}(g, v, v_\ell)$ is a safety vehicle deceleration.

C. Physics of traffic flow model

The physics of model (2)–(4) is as follows:

(i) In Eq. (2), in addition to driver overacceleration (1), there is function $K_{\Delta v}\Delta v$ [29–32,42] that describes vehicle speed adaptation to the speed of the preceding vehicle v_ℓ occurring independently of space gap g within the space-gap range $g_{\text{safe}} \leqslant g \leqslant G$. Thus, a decrease in the speed of the preceding vehicle v_ℓ does not lead to a stronger decrease in the speed v: No driver overreaction occurs.

(ii) Equation (3) describes vehicle acceleration at large space gaps $g > G$.

(iii) Contrary to driver overacceleration a_{OA} (1) applied in Eq. (2), function $K_{\Delta v}\Delta v$ in Eq. (2) at $\Delta v > 0$ and Eq. (3) describe "usual" driver acceleration that does not show a discontinuous character.

(iv) Equation (4) describes safety vehicle deceleration that should prevent collisions between vehicles at small space gaps $g < g_{\text{safe}}$; contrary to Eq. (2), safety vehicle deceleration $a_{\text{safety}}(g, v, v_\ell)$ in Eq. (4) can lead to driver overreaction. There are many concepts developed in standard traffic flow models [1–28] that can be used for safety vehicle deceleration $a_{\text{safety}}(g, v, v_\ell)$. For simulations below, we use one of them described by Helly's function [8]

$$a_{\text{safety}}(g, v, v_\ell) = K_1(g - g_{\text{safe}}) + K_2\Delta v, \tag{5}$$

where K_1 and K_2 are positive dynamic coefficients[3].

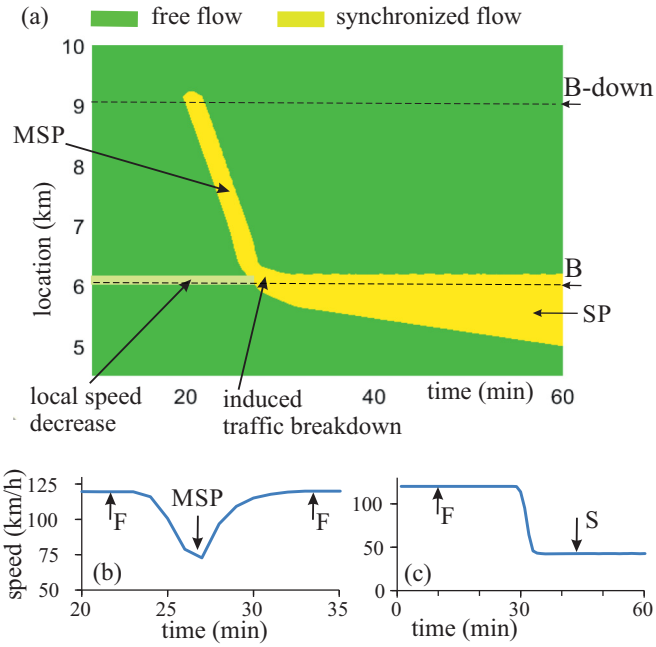

FIG. 3. Simulations with model (2)–(5) of nucleation nature of traffic breakdown on a single-lane road of length $L = 10$ km with two identical on-ramp bottlenecks B and B-down at locations $x = x_{\text{on,B}} = 6$ km and $x = x_{\text{on,B-down}} = 9$ km, respectively. (a) Speed data presented in space and time as made in Fig. 1(a). (b), (c) Averaged (1-min) speeds at $x = 7$ km within MSP (b) and at $x = 5.7$ km (c) within a synchronized flow pattern (SP) induced through MSP propagation at bottleneck B. Flow rate in free flow on the road at $x = 0$ is $q_{\text{in}} = 2250$ vehicles/h. Bottleneck model is the same as that in [45]: there is a merging region of length $L_{\text{m}} = 0.3$ km; vehicles merge at a middle location between vehicles on the road at the preceding vehicle speed v^+ when $g > g_{\text{target}}^{(\min)} = \lambda_{\text{b}}v^+ + d$ with $\lambda_{\text{b}} = 0.3$ s; on-ramp inflow rates are $q_{\text{on,B-down}} = 0$ and $q_{\text{on,B}} = 685$ vehicles/h; to induce the MSP at bottleneck B-down, impulse $q_{\text{on,B-down}} = 400$ vehicles/h at $t = 20$ min during 2 min has been applied. Vehicles are identical ones with the following parameters: $a_{\max} = 2.5$ m/s^2, $\alpha = 1$ m/s^2, $K_{\Delta v} = 0.8$ s^{-1}, $K_1 = 0.15$ s^{-2}, $K_2 = 0.95$ s^{-1}. Under conditions $0 \leqslant v \leqslant v_{\text{free}}$, vehicle motion is found from equations $dv/dt = a$, $dx/dt = v$ solved with the second-order Runge-Kutta method with time step 10^{-2} s. In panels (b) and (c), F and S are states of free flow and synchronized flow, respectively. Other model parameters are the same as those in Fig. 2.

As often assumed, drivers cannot estimate space gaps very well. A misjudgment of the headway leads often to hard braking that can lead to driver overreactions. The same is true for the speed difference between vehicles. Driver reaction on short space gaps and large speed differences are simulated in model (2)–(5) as follows. If the space gap g becomes smaller than safe space gap g_{safe}, this leads to hard braking described by Eq. (5). Hard braking can lead to driver overreaction, but it should not necessarily lead to driver overreaction; this depends on values K_1 and K_2 in (5). When the speed difference causes hard braking, this can also lead to driver overreaction, but it should not necessarily lead to driver overreaction. In simulations of model (2)–(5) (Figs. 3–7), we have chosen values K_1 and K_2 at which no driver overreaction occurs.

[3]Contrary to [44], in model (2)–(5) *no* different states (like optimistic state or defensive state of [44]) are assumed in collision-free traffic dynamics governed by safety vehicle deceleration.

III. NUCLEATION NATURE OF TRAFFIC BREAKDOWN (F → S TRANSITION)

We have shown that if we choose coefficients K_1 and K_2 in (5) (Fig. 3) at which even at $g \leqslant g_{\text{safe}}$ no driver overreaction occurs in model (2)–(5), then, nevertheless, this model shows all known empirical nucleation features of traffic breakdown [Fig. 1(a)]: A moving synchronized flow pattern (MSP) induced at downstream bottleneck B-down propagates upstream. While reaching upstream bottleneck B, the MSP induces F → S transition at the bottleneck [Fig. 3(a)].

Formula (1) for driver overacceleration explains induced traffic breakdown (induced F → S transition) as follows. Due to a vehicle merging from the on-ramp, condition $g < g_{\text{safe}}$ can be satisfied resulting in vehicle deceleration. As a result of this vehicle deceleration, a local speed decrease occurs at bottleneck B [labeled by "local speed decrease" in Fig. 3(a)]. The minimum speed $v_{\text{min}}^{(\text{dec})}$ within the local speed decrease satisfies condition $v_{\text{min}}^{(\text{dec})} > v_{\text{syn}}$. Therefore, according to (1), vehicles accelerate with overacceleration $a_{\text{OA}} = \alpha$ from the local speed decrease; this prevents congestion propagation upstream of bottleneck B. Contrarily, the minimum speed within the MSP satisfies condition $v_{\text{min}}^{(\text{MSP})} < v_{\text{syn}}$ [Fig. 3(b)]. Then, according to (1), driver overacceleration $a_{\text{OA}} = 0$: When the MSP reaches bottleneck B, synchronized flow is induced. A synchronized flow pattern (SP) resulting from induced traffic breakdown remains at bottleneck B. This is because the speed within the SP is less than the speed v_{syn} in (1) [Fig. 3(c)] and, therefore, driver overacceleration $a_{\text{OA}} = 0$.

It should be noted that because the deceleration capabilities of a car are much higher than the acceleration capabilities, for simulations of the F → S transition in Fig. 3(a) we have used a relatively small maximum driver overacceleration $\alpha = 1$ m/s^2. This choice should show that already a small driver overacceleration can explain the nucleation of traffic breakdown (F → S transition). Simulations made show that the choice of a larger driver overacceleration [for the maximum driver overacceleration α in Eq. (1) we have used values between 1 and 2.5 m/s^2] does not qualitatively change results presented in Fig. 3.

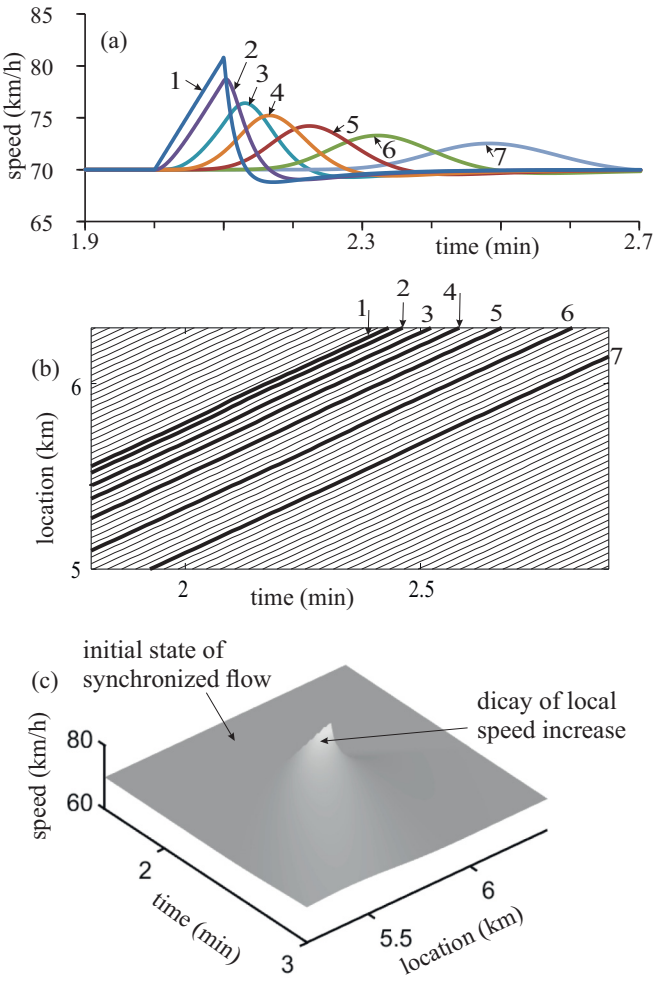

FIG. 4. Nucleation character of S → F instability: No S → F instability occurs. Simulations with model (2)–(5) made on single-lane road of length 8 km without bottlenecks with initial homogeneous synchronized flow state at $v = 70$ km/h and $g = 27.5$ m. (a), (b) Time development of speeds (a) and trajectories (b) of vehicles 1–7 caused by initial local speed increase of vehicle 1 simulated through short-time acceleration of vehicle 1 with $a = 0.5$m/s^2 during 6.5 s. (c) Spatiotemporal development of the vehicle speed during the decay of the initial local increase in the speed of vehicle 1 in (a). Other model parameters are the same as those in Figs. 2 and 3.

IV. NUCLEATION NATURE OF S → F INSTABILITY

Formula (1) for driver overacceleration explains also the S → F instability. We consider the time development of a local speed increase in an initial homogeneous state of synchronized flow (Figs. 4 and 5). The cause of the local speed increase is a short-time acceleration of one of the vehicles (vehicle 1 in Fig. 4 or vehicle 8 in Fig. 5) occurring within the same initial homogeneous state of synchronized flow in Figs. 4 and 5. Vehicle 1 (Fig. 4) and vehicle 8 (Fig. 5) have to decelerate later to the speed of the preceding vehicle moving at the initial synchronized flow speed ($v = 70$ km/h in Figs. 4 and 5).

It has been found that there are two possibilities:

(i) The increase in the speed of following vehicles (vehicles 2–7 in Fig. 4) decays over time (Fig. 4). This decay of the initial local speed increase occurs when the maximum speed of vehicle 2 ($v_{\text{max}}^{(2)} = 77.9$ km/h) that follows vehicle 1 is less than the critical speed v_{syn} in (1). Therefore, driver overacceleration is equal to $a_{\text{OA}} = 0$. Because there is no driver overacceleration, the initial local speed increase in synchronized flow decays over time.

(ii) Contrarily, if vehicle 8 (Fig. 5) accelerates only 0.5 s longer than vehicle 1 (Fig. 4), the local speed increase initiated by vehicle 8 grows over time [vehicles 9–14 in Figs. 5(a) and 5(b)] leading to the S → F instability (Fig. 5). The S → F instability occurs because the maximum speed of vehicle 9 ($v_{\text{max}}^{(9)} = 81.9$ km/h) that follows vehicle 8 is higher than the critical speed v_{syn} in (1). Therefore, driver overacceleration is equal to $a_{\text{OA}} = \alpha$. The driver overacceleration causes the S → F instability. The time development of the S → F instability leads to a local S → F transition in the initial synchronized flow [Fig. 5(c)].

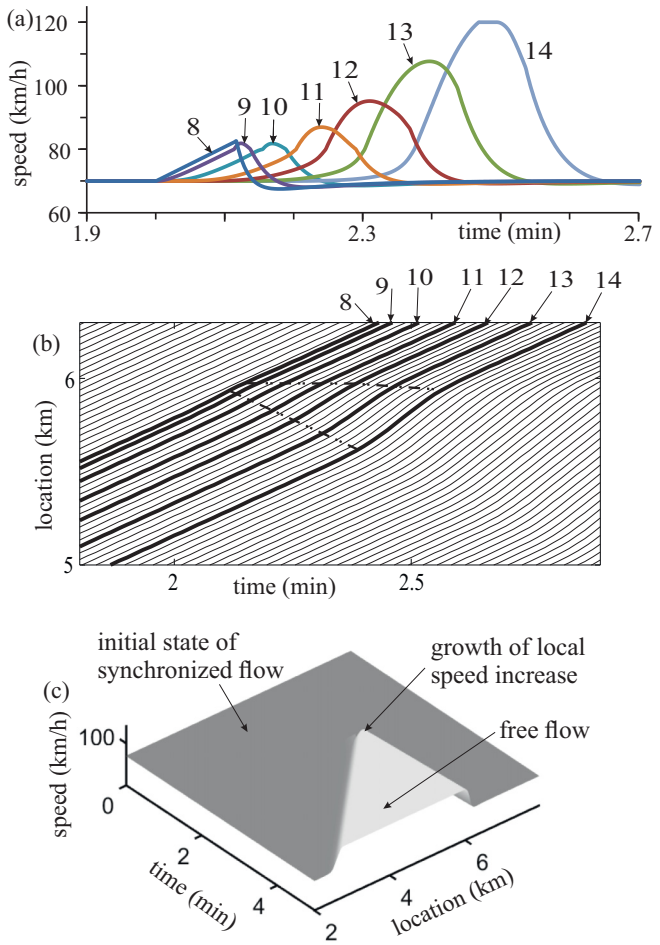

FIG. 5. Nucleation character of S → F instability: S → F instability occurs. Simulations with model (2)–(5) made at the same model parameters as those in Fig. 4, in particular, at $v = 70$ km/h and $g = 27.5$ m in initial homogeneous synchronized flow state; however, in comparison with Fig. 4 there is only one exception: The duration of short-time acceleration of vehicle 8 with $a = 0.5$ m/s^2 is equal to 7 s, i.e., the initial acceleration of vehicle 8, which causes the local speed increase in synchronized flow, is 0.5 s longer than that of vehicle 1 in Fig. 4. In (a) and (b) time development of speeds (a) and trajectories (b) of vehicles 8–14. (c) Spatiotemporal development of speed during S → F instability shown in (a) and (b). Dashed-dotted curves in (b) denote the development of S → F instability in synchronized flow leading to the S → F transition. Other model parameters are the same as those in Figs. 2–4.

V. RANGE OF HIGHWAY CAPACITIES AND TRAFFIC PATTERNS RESULTING FROM BREAKDOWN

Formula (1) for driver overacceleration explains also the range of highway capacities of three-phase traffic theory [29–32,42] (Fig. 6):

(i) Free flow is metastable with respect to traffic breakdown at the bottleneck when $C_{\min} \leqslant q_{\text{sum}} < C_{\max}$, where $q_{\text{sum}} = q_{\text{in}} + q_{\text{on}}$; q_{in} is the flow rate in free flow on the road upstream of the bottleneck, q_{on} is the on-ramp inflow rate; $C_{\min}$ and $C_{\max}$ are minimum and maximum highway capacities, respectively. Under condition $C_{\min} \leqslant q_{\text{sum}} < C_{\max}$, traffic breakdown (F → S transition) can be induced at the bottleneck.

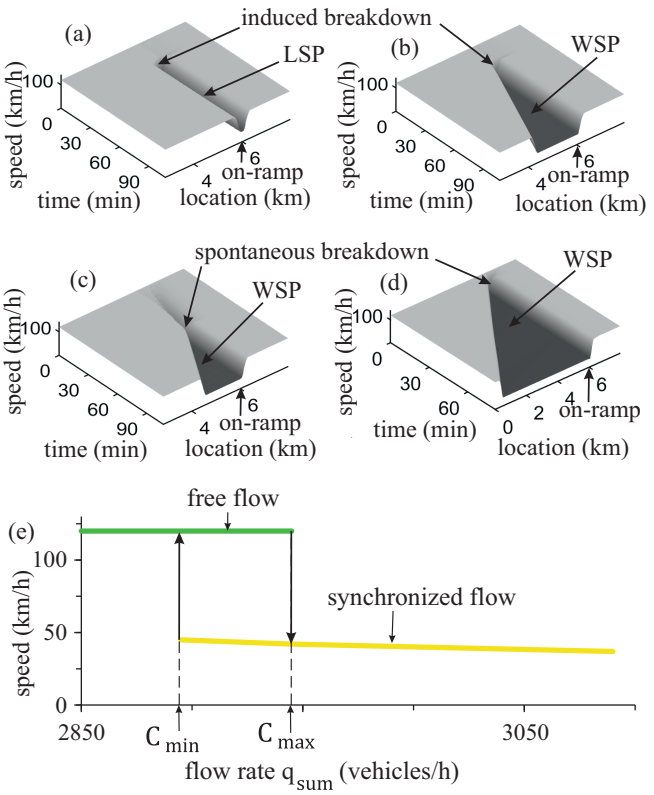

FIG. 6. Simulations with model (2)–(5) of traffic congested patterns resulting from traffic breakdown on a single-lane road of length 8 km with on-ramp bottleneck at 6 km at the same flow rate $q_{\text{in}} = 2250$ vehicles/h as that in Fig. 3. (a)–(d) Speed in space and time: (a) $q_{\text{on}} = q_{\text{on,min}} = 645$ vehicles/h, (b) $q_{\text{on}} = 680$ vehicles/h, (c) $q_{\text{on}} = q_{\text{on,max}} = 695$ vehicles/h, (d) $q_{\text{on}} = 840$ vehicles/h; $q_{\text{on,min}} = C_{\min} - q_{\text{in}}$, $C_{\min} = 2895$ vehicles/h (a); $q_{\text{on,max}} = C_{\max} - q_{\text{in}}$, $C_{\max} = 2945$ vehicles/h (c). (e) Range of highway capacities: The speed in free flow and the mean speed in synchronized flow within the SPs in panels (a), (b), (c), and (d) as functions of the total flow rate in free flow at the bottleneck q_{sum}. In (a) and (b), traffic breakdown has been induced at $t = 20$ min by on-ramp inflow impulse $\Delta q_{\text{on}} = 355$ vehicles/h (a) and 320 vehicles/h (b) of 2 min (a) and 1 min (b) duration. LSP is a localized SP; WSP is a widening SP. Other parameters are the same as those in Figs. 2 and 3.

(ii) When $q_{\text{sum}} < C_{\min}$, no traffic breakdown can be induced: Any initial short-time disturbance in free flow at the bottleneck decays over time.

(iii) At $q_{\text{sum}} = C_{\min}$, a congested pattern resulting from induced traffic breakdown is a localized SP (LSP) [Fig. 6(a)]: The LSP width (in the longitudinal direction) does not increase over time.

(iv) When at a given q_{in} and $q_{\text{sum}} > C_{\min}$ the on-ramp inflow rate q_{on} increases, a widening SP (WSP) results from induced traffic breakdown [Fig. 6(b)]: The WSP width increases over time.

(v) At $q_{\text{sum}} = C_{\max}$, after a time delay, spontaneous traffic breakdown at the bottleneck occurs [Fig. 6(c)]. At a given q_{in} and $q_{\text{sum}} > C_{\max}$, the more the on-ramp inflow rate q_{on} exceeds a maximum on-ramp inflow rate $q_{\text{on,max}} = C_{\max} - q_{\text{in}}$, the shorter the time delay of spontaneous traffic breakdown [Figs. 6(c) and 6(d)].

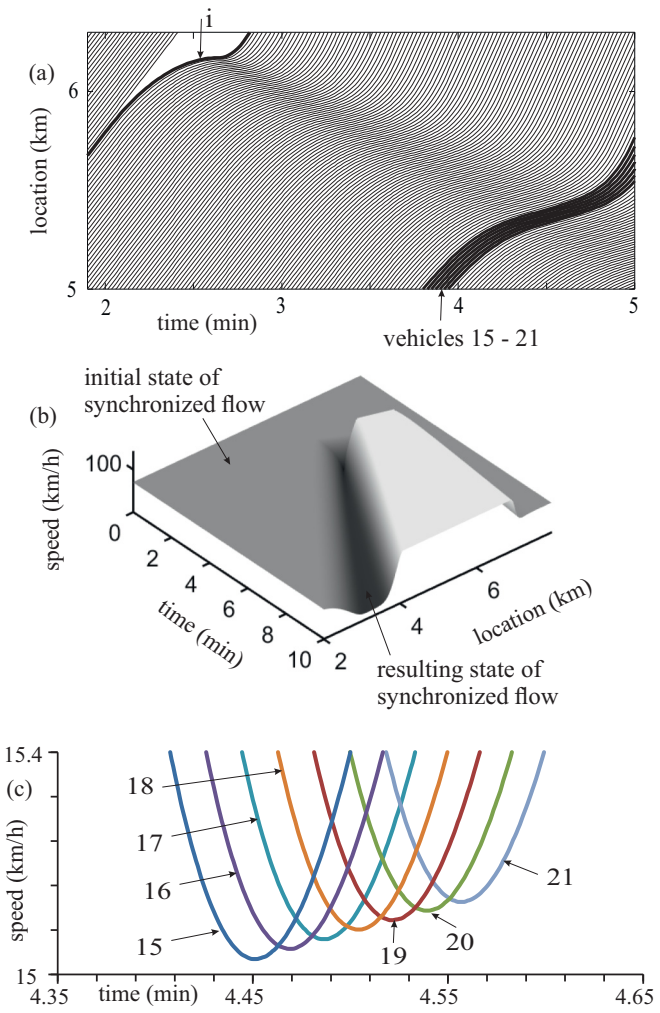

FIG. 7. Absence of driver overreaction in model (2)–(5) under parameters used in Figs. 2 and 3. Simulations made on single-lane road of length 8 km without bottlenecks with initial homogeneous state of synchronized flow with $v = 70$ km/h and $g = g_{\text{safe}} = 19.5$ m: Time development of vehicle trajectories (a), speed in space and time (b), and speeds of a sequence of vehicles 15–21 caused by initial local speed decrease of vehicle i in (a) simulated through deceleration of vehicle i with $a = -0.5$ m/s^2 to the speed $v = 0$; vehicle i remains stationary for 1 s and then accelerates.

(vi) In general, the larger the on-ramp inflow rate q_{on} (at a given q_{in}), the lower the mean synchronized flow speed within the SP [Fig. 6(e)].

VI. ABSENT OF DRIVER OVERREACTION IN TRAFFIC FLOW MODEL

We have found that in model (2)–(5) under parameters used in Figs. 2 and 3 there is no driver overreaction on the deceleration of the preceding vehicle even at the smallest possible space gap between vehicles $g = g_{\text{safe}}$ in an initial homogeneous state of traffic flow.

In Fig. 7 under condition $g = g_{\text{safe}}$ in an initial homogeneous synchronized flow, vehicle i decelerates to a standstill, remains stationary for 1 s, and then accelerates. It turns out that none of the following vehicles decelerate to the standstill. The minimum speed of the following vehicles increases slowly over time [vehicles 15–21 in Fig. 7(c)]. Finally, rather than a wide moving jam, a state of synchronized flow with a lower speed $v \approx 15.5$ km/h [labeled by "resulting state of synchronized flow" in Fig. 7(b)] results from the deceleration of vehicle i.

VII. BEHAVIORAL ORIGIN OF DRIVER OVERACCELERATION IN ROAD LANE

As is well known [1–28], the behavioral origin of driver overreaction is related to the wish of drivers to avoid vehicle collisions. Contrarily, the behavioral origin of driver overacceleration is related to the wish of drivers to move in free flow. To understand the origin of the discontinuous character of driver overacceleration, first recall that as formulated in (2), space gap g can be larger than safe space gap g_{safe}.

(i) We consider a driver that reaches the local speed decrease at the bottleneck (bottleneck B in Fig. 3(a)). This is realized during time interval, when the MSP is still far enough downstream of the bottleneck [Fig. 3(a)]. We assume that the driver accelerates (overacceleration occurs, i.e., $a_{\text{OA}} = \alpha$) trying to escape from the local speed decrease. This driver overacceleration, which prevents upstream propagation of the local speed decrease at the bottleneck, is possible at the cost of the decrease in the space gap (as long as $g > g_{\text{safe}}$) and only when the local speed decrease at the bottleneck is still low enough. Contrarily, when the MSP has already reached the bottleneck, dense synchronized flow of a low enough speed is at the bottleneck. Then we assume that drivers recognize that there is no possibility to escape from this synchronized flow; therefore, no driver overacceleration is realized, i.e., $a_{\text{OA}} = 0$.

(ii) We assume that a driver can randomly accelerate in synchronized flow leading to a local speed increase in the synchronized flow (Figs. 4 and 5). Model (2)–(5) is deterministic. For this reason, the random local speed increase is simulated through time-limited acceleration of a vehicle (vehicle 1 in Fig. 4 or vehicle 8 in Fig. 5). This vehicle acceleration leads to acceleration of the following vehicles (vehicles 2–7 or vehicles 9–14, respectively, in Figs. 4 and 5). When in initial homogeneous synchronized flow the space gap $g > g_{\text{safe}}$ and the synchronized flow speed is not very low (in Figs. 4 and 5, speed $v = 70$ km/h and space gap $g = 27.5$ m, whereas safe space gap $g_{\text{safe}} = 19.5$ m), we assume that there can be two possibilities for the development of the initial local speed increase in synchronized flow:

First possibility. The initial local speed increase in synchronized flow is not large enough [Fig. 4(a)]. Then we assume that the following drivers are not motivated for strong acceleration because the drivers recognize that there is no possibility to escape from synchronized flow (no driver overacceleration is realized, i.e., $a_{\text{OA}} = 0$). If this occurs, the initial local speed increase decays (Fig. 4).

Second possibility. The initial local speed increase in synchronized flow is larger than some critical value [Fig. 5(a)]. Then we assume that the following drivers are motivated for strong acceleration, because the drivers recognize that there is a possibility to escape from synchronized flow. As a result of this strong driver acceleration, the vehicle

speed becomes larger than the speed of the preceding vehicle (driver overacceleration occurs, i.e., $a_{OA} = \alpha$). If this driver overacceleration is realized for the following vehicles, then the S → F instability occurs (Fig. 5).

As defined in three-phase traffic theory, overacceleration is vehicle acceleration that exhibits the discontinuous character when free flow transforms into synchronized flow [Figs. 1(b) and 1(c)]. However, the prefix *over* in the term *overacceleration* literally implies too much acceleration. The choice of the term *overacceleration* can be understood if we consider the S→F instability: In this case, overacceleration is a stronger vehicle acceleration than it is needed for car-following in the initial synchronized flow. Indeed, due to overacceleration the speed of the following vehicle becomes *higher* than the speed of the preceding vehicle.

As emphasized, the behavioral origin of overacceleration is related to the wish of drivers to move in free flow. Contrarily, the behavioral origin of vehicle overdeceleration caused by driver overreaction on deceleration of the preceding vehicle is related to the wish of the drivers to avoid vehicle collisions. This totally different physics of overacceleration and overdeceleration can nevertheless be used for some addition explanation of the choice of the term *overacceleration*: Due to overacceleration the speed of the following vehicle becomes *higher* than the speed of the preceding vehicle; contrary to overacceleration, due to overdeceleration the speed of the following vehicle becomes *less* than the speed of the preceding vehicle.

VIII. DISCUSSION

A. Comparison of simulations of model of overacceleration with empirical traffic data

We have shown that a traffic flow model that incorporates a discontinuity in driver overacceleration (1) [Fig. 2(a)] can indeed show and explain the nucleation nature of traffic breakdown (F → S transition) at a highway bottleneck [Fig. 3(a)] without the effect of driver overreaction. The nucleation character of traffic breakdown (F → S transition) at bottlenecks is often observed in real field (empirical) traffic data measured on highways [Fig. 1(a)] (see other empirical examples in [31,32]).

This traffic flow model (2)–(5), in which no driver overreaction is realized, show also SPs resulting from traffic breakdown, like LSP [Fig. 6(a)] and different WSPs [Figs. 6(b)–6(d)]. LSPs and WSPs have been observed in a huge number of empirical traffic data (see, e.g., [29–33]).

Currently, there are many available microscopic empirical data measured through probe vehicles (see, e.g., [32,33]). In the probe vehicle data, empirical S→F transitions within synchronized flow have been observed (see, e.g., Fig. 26 of Ref. [43]). However, the microscopic traffic data are related to a small share of probe vehicles moving in traffic flow (about 3–5%). For this reason, such empirical microscopic traffic data cannot be used for a study of the S → F instability that model (2)–(5) shows (Fig. 5): For the resolving of the S → F instability in empirical data, almost all empirical vehicle trajectories in traffic flow are needed to be measured. Unfortunately, suitable microscopic empirical data, which can be used for empirical studies of the S → F instability, are not currently available; empirical studies of the S → F instability can be an interesting task for further investigations.

Another result of simulations of model (2)–(5), in which no driver overreaction occurs, is as follows: Independent of the flow rate at the bottleneck, no moving jams emerge within SPs resulting from traffic breakdown (Fig. 6). This contradicts to both the three-phase traffic theory and empirical results

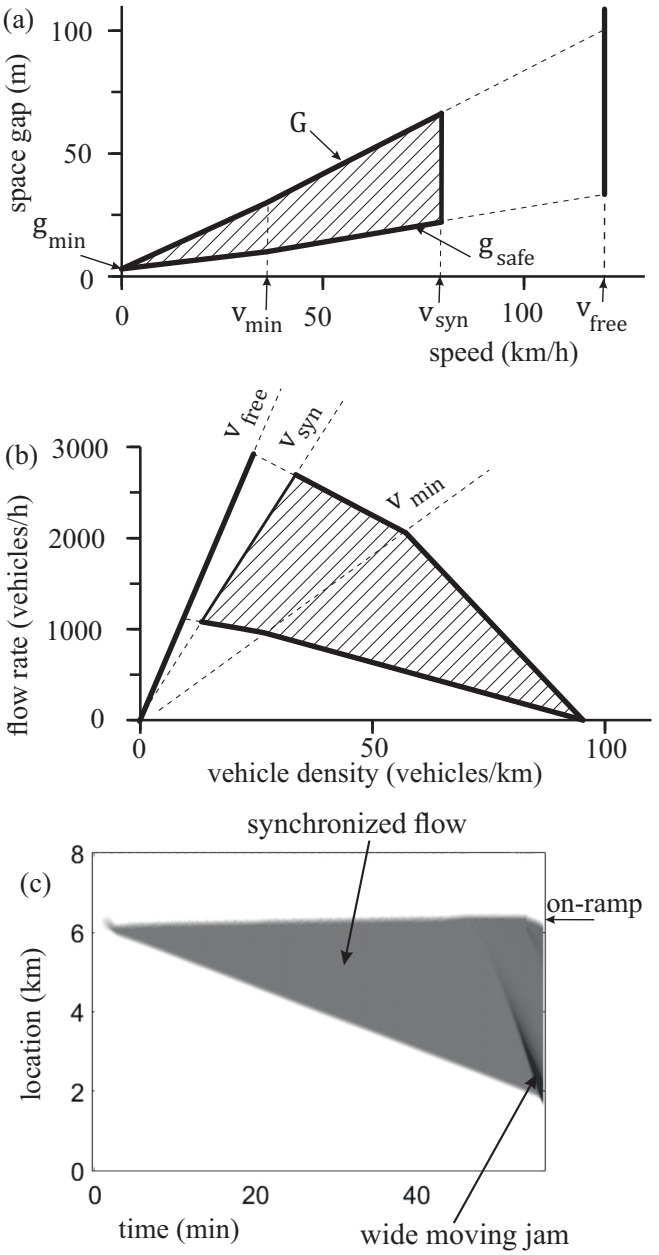

FIG. 8. Simulations of model (2)–(7) with $v_{min} = 36$ km/h, $g_{min} = 3$ m on single-lane road of length 8 km with on-ramp bottleneck at 6 km at the same flow rate $q_{in} = 2250$ vehicles/h as that in Fig. 3. (a, b) Model steady states in space-gap–speed (a) and flow–density (b) planes (dashed 2D-regions are related to steady states of synchronized flow). (c) Speed data in space and time presented by regions with variable shades of gray [shades of gray vary from white to black when the speed decreases from 120 km/h (white) to 0 km/h (black)]; $q_{on} = 875$ vehicles/h. Other parameters are the same as those in Figs. 2 and 3.

(see, e.g., [29–33]), in which wide moving jams emerge in synchronized flow at a low enough synchronized flow speed; the moving jams are also called "stop-and-go" traffic patterns (see, e.g., [21,27]). For this reason, we can assume that the emergence of wide moving jams in synchronized flow (S → J transition) is caused by driver overreaction in synchronized flow, i.e., by the classical traffic flow instability in synchronized flow: Because no driver overreaction occurs in model (2)–(5), this model cannot show the classical traffic flow instability and S → J transitions resulting from the development of the classical instability. This assumption will be supported in the next subsection.

B. Effect of driver overreaction: Emergence of wide moving jam in synchronized flow

Up to now we have studied traffic flow model (2)–(5) at such model parameters at which no driver overreaction occurs. Clearly, at other model parameters in (2)–(5) as those used in Figs. 2–7 driver overreaction can occur. This case is illustrated in the following example.

As known, when the vehicle speed $v \to 0$, safe space gap g_{safe} should tend to a minimum space gap $g_{\min}$. Respectively, in (2)–(5), rather than $g_{\text{safe}} = v\tau_{\text{safe}}$ and $G = v\tau_{\text{G}}$ [Figs. 2(b) and 2(c) and 3], we get

$$g_{\text{safe}} = \begin{cases} v\tau_{\text{safe}} & \text{at} \quad v \geqslant v_{\min} \\ g_{\min} + v(\tau_{\text{safe}} - \tau_{\min}) & \text{at} \quad v < v_{\min}, \end{cases} \tag{6}$$

$$G = \begin{cases} v\tau_{\text{G}} & \text{at} \quad v \geqslant v_{\min} \\ g_{\min} + v(\tau_{\text{G}} - \tau_{\min}) & \text{at} \quad v < v_{\min}, \end{cases} \tag{7}$$

where $\tau_{\min} = g_{\min}/v_{\min}$; $g_{\min}$ and $v_{\min}$ (where $v_{\min} < v_{\text{syn}}$) are parameters [Figs. 8(a) and 8(b)]. Model (2)–(7) shows results of three-phase traffic theory [29–32,42] [Fig. 8(c)]:

(i) Traffic breakdown (F → S transition) is caused by driver overacceleration.

(ii) When within SPs resulting from traffic breakdown the synchronized flow speed denoted by v_{S} satisfies condition $v_{\text{S}} > v_{\min}$, no classical traffic instability and, therefore, no moving jams occurs within SPs. This result is explained as follows: At $v \geqslant v_{\min}$ and under the same other parameters as those used in Figs. 2 and 3, model (2)–(5) and model (2)–(7) are identical models, i.e., no driver overreaction occurs in both models. The synchronized flow speed v_{S} within each of the SPs shown in Fig. 6 satisfies condition $v_{\text{S}} > v_{\min}$. For this reason, all results presented in Fig. 6 for model (2)–(5) remain also the same ones for model (2)–(7).

(iii) Only when the synchronized flow speed v_{S} within an SP is low enough, specifically, the speed satisfies condition $v_{\text{S}} < v_{\min}$ [Fig. 8(c)], as we have found, driver overreaction can occur within synchronized flow. As a result, at a large enough flow rate at the bottleneck, at which the synchronized flow speed v_{S} within the SP satisfies condition $v_{\text{S}} < v_{\min}$, model (2)–(7) shows the classical traffic instability caused by driver overreaction within the SP leading to wide moving jam emergence in synchronized flow [labeled by "wide moving jam" in Fig. 8(c)].

Therefore, simulations of model (2)–(7) show that traffic breakdown (F → S transition) occurs at the bottleneck solely due to the discontinuity in driver overacceleration (1), i.e., without the effect of driver overreaction. Contrary to traffic breakdown (F → S transition), wide moving jam emergence in synchronized flow (S → J transition) results from driver overreaction occurring in synchronized flow at a low enough synchronized flow speed.

C. Conclusions

The main conclusion of this paper is as follows:

– A model of driver overacceleration (1) used in traffic flow model (2)–(5), in which no driver overreaction occurs, explains the empirical nucleation nature of traffic breakdown through driver overacceleration.

In the paper we have proven that the mechanism of driver overacceleration (1) explains the empirical nucleation nature of traffic breakdown (F → S transition) at bottlenecks. Further applications of driver overacceleration model (1) for the development of other traffic models (like cellular automaton traffic flow models) as well as for studies of other vehicular traffic phenomena that are out of the scope of this paper can be an interesting task for scientific investigations.

ACKNOWLEDGMENTS

I thank Sergey Klenov for help in simulations and useful suggestions. I thank our partners for their support in the project "LUKAS–Lokales Umfeldmodell für das Kooperative, Automatisierte Fahren in komplexen Verkehrssituationen" funded by the German Federal Ministry for Economic Affairs and Climate Action.

[1] R. E. Chandler, R. Herman, and E. W. Montroll, Oper. Res. **6**, 165 (1958).
[2] R. Herman, E. W. Montroll, R. B. Potts, and R. W. Rothery, Oper. Res. **7**, 86 (1959).
[3] D. C. Gazis, R. Herman, and R. B. Potts, Oper. Res. **7**, 499 (1959).
[4] D. C. Gazis, R. Herman, and R. W. Rothery, Oper. Res. **9**, 545 (1961).
[5] E. Kometani and T. Sasaki, J. Oper. Res. Soc. Jap. **2**, 11 (1958).
[6] E. Kometani and T. Sasaki, Oper. Res. **7**, 704 (1959).
[7] E. Kometani and T. Sasaki, Oper. Res. Soc. Jap. **3**, 176 (1961).
[8] W. Helly, *Proceedings of the Symposium on Theory of Traffic Flow, Research Laboratories, General Motors* (Elsevier, Amsterdam, 1959), pp. 207–238.
[9] G. F. Newell, Oper. Res. **9**, 209 (1961); Transp. Res. B **36**, 195 (2002).
[10] P. G. Gipps, Transp. Res. B **15**, 105 (1981); **20**, 403 (1986).
[11] R. Wiedemann, *Simulation des Straßenverkehrsflusses* (University of Karlsruhe, Karlsruhe, 1974).
[12] K. Nagel and M. Schreckenberg, J. Phys. I France **2**, 2221 (1992).
[13] M. Bando, K. Hasebe, A. Nakayama, A. Shibata, and Y. Sugiyama, Phys. Rev. E **51**, 1035 (1995).

[14] S. Krauss, P. Wagner, and C. Gawron, Phys. Rev. E **55**, 5597 (1997).
[15] R. Barlović, L. Santen, A. Schadschneider, and M. Schreckenberg, Eur. Phys. J. B **5**, 793 (1998).
[16] T. Nagatani, Physica A **261**, 599 (1998); Phys. Rev. E **59**, 4857 (1999).
[17] M. Treiber, A. Hennecke, and D. Helbing, Phys. Rev. E **62**, 1805 (2000).
[18] B. S. Kerner and P. Konhäuser, Phys. Rev. E **48**, R2335 (1993); **50**, 54 (1994); B. S. Kerner, P. Konhäuser, and M. Schilke, *ibid.* **51**, 6243 (1995).
[19] N. H. Gartner, C. J. Messer, and A. Rathi, *Traffic Flow Theory* (Transportation Research Board, Washington, DC, 2001).
[20] J. Barceló, *Fundamentals of Traffic Simulation* (Springer, Berlin, 2010).
[21] L. Elefteriadou, *An Introduction to Traffic Flow Theory*, Springer Optimization and Its Applications Vol. 84 (Springer, Berlin, 2014).
[22] D. Ni, *Traffic Flow Theory* (Elsevier, Amsterdam, 2015).
[23] D. Chowdhury, L. Santen, and A. Schadschneider, Phys. Rep. **329**, 199 (2000).
[24] D. Helbing, Rev. Mod. Phys. **73**, 1067 (2001).
[25] T. Nagatani, Rep. Prog. Phys. **65**, 1331 (2002).
[26] K. Nagel, P. Wagner, and R. Woesler, Oper. Res. **51**, 681 (2003).
[27] M. Treiber and A. Kesting, *Traffic Flow Dynamics* (Springer, Berlin, 2013).
[28] A. Schadschneider, D. Chowdhury, and K. Nishinari, *Stochastic Transport in Complex Systems* (Elsevier Science, New York, 2011).
[29] B. S. Kerner, *The Physics of Traffic* (Springer, Berlin, New York, 2004).
[30] B. S. Kerner, *Introduction to Modern Traffic Flow Theory and Control* (Springer, Berlin, 2009).
[31] B. S. Kerner, *Breakdown in Traffic Networks* (Springer, Berlin/New York, 2017).
[32] B. S. Kerner, *Understanding Real Traffic* (Springer, Cham, 2021).
[33] H. Rehborn, M. Koller, and S. Kaufmann, *Data-Driven Traffic Engineering* (Elsevier, Amsterdam, 2021).
[34] B. S. Kerner, H. Rehborn, R.-P. Schäfer, S. L. Klenov, J. Palmer, S. Lorkowski, and N. Witte, Physica A **392**, 221 (2013).
[35] M. J. Lighthill and G. B. Whitham, Proc. Roy. Soc. A **229**, 317 (1955).
[36] P. I. Richards, Oper. Res. **4**, 42 (1956).
[37] A. D. May, *Traffic Flow Fundamentals* (Prentice-Hall, Hoboken, NJ, 1990).
[38] C. F. Daganzo, Transp. Res. B **28**, 269 (1994); **29**, 79 (1995).
[39] *Highway Capacity Manual*, 6th ed., National Research Council (Transportation Research Board, Washington, DC, 2016).
[40] B. S. Kerner, Phys. World **12**, 25 (1999); Trans. Res. Rec. **1678**, 160 (1999); J. Phys. A: Math. Gen. **33**, L221 (2000); Phys. Rev. E **65**, 046138 (2002); Net. Spat. Econ. **1**, 35 (2001); Math. Comput. Model. **35**, 481 (2002).
[41] B. S. Kerner, Phys. Rev. E **92**, 062827 (2015).
[42] B. S. Kerner and S. L. Klenov, J. Phys. A: Math. Gen. **35**, L31 (2002); Phys. Rev. E **68**, 036130 (2003); J. Phys. A: Math. Gen. **39**, 1775 (2006); Phys. Rev. E **80**, 056101 (2009); J. Phys. A: Math. Theor. **43**, 425101 (2010); B. S. Kerner, S. L. Klenov, and D. E. Wolf, J. Phys. A: Math. Gen. **35**, 9971 (2002); B. S. Kerner, S. L. Klenov, and M. Schreckenberg, Phys. Rev. E **84**, 046110 (2011); **89**, 052807 (2014); B. S. Kerner, *ibid.* **85**, 036110 (2012); Europhys. Lett. **102**, 28010 (2013); B. S. Kerner, S. L. Klenov, and M. Schreckenberg, Physica A **397**, 76 (2014); B. S. Kerner, S. L. Klenov, G. Hermanns, and M. Schreckenberg, *ibid.* **392**, 4083 (2013).
[43] B. S. Kerner, Phys. Rev. E **100**, 012303 (2019).
[44] H. K. Lee, R. Barlović, M. Schreckenberg, and D. Kim, Phys. Rev. Lett. **92**, 238702 (2004).
[45] B. S. Kerner, Phys. Rev. E **108**, 014302 (2023).